HHS Public Access

Author manuscript

Health Phys. Author manuscript; available in PMC 2021 November 01.

Published in final edited form as:

Health Phys. 2020 November ; 119(5): 594–603. doi:10.1097/HP.0000000000001348.

Evaluation of plasma biomarker utility for the gastrointestinal acute radiation syndrome in non-human primate after partial body irradiation with minimal bone marrow sparing through correlation with tissue and histological analyses

Praveen Kumar[1,+], **Pengcheng Wang**[1,+], **Gregory Tudor**[2], **Catherine Booth**[2], **Ann M. Farese**[3], **Thomas J. MacVittie**[3], **Maureen A Kane**[1]

[1]University of Maryland, School of Pharmacy, Department of Pharmaceutical Sciences, Baltimore, MD, USA.

[2]Epistem Ltd., Manchester, UK;

[3]University of Maryland, School of Medicine, Department of Radiation Oncology, Baltimore, MD 21201

Abstract

Exposure to total- and partial-body irradiation following a nuclear or radiological incident result in the potentially lethal acute radiation syndromes of the gastrointestinal and hematopoietic systems in a dose-and time-dependent manner. Radiation-induced damage to the gastrointestinal tract is observed within days to weeks post-irradiation. Our objective in this study was to evaluate plasma biomarker utility for the gastrointestinal acute radiation syndrome in non-human primate after partial body irradiation with minimal bone marrow sparing through correlation with tissue and histological analyses. Plasma and jejunum samples from non-human primates exposed to partial body irradiation of 12 Gy with bone marrow sparing of 2.5% were evaluated at various time points from day 0 to day 21 as part of a natural history study. Additionally, longitudinal plasma samples from non-human primates exposed to 10 Gy partial body irradiation with 2.5% bone marrow sparing were evaluated at timepoints out to 180 days post-irradiation. Plasma and jejunum metabolites were quantified via liquid chromatography - tandem mass spectrometry and histological analysis consisted of corrected crypt number, an established metric to assess radiation-induced gastrointestinal damage. A positive correlation of metabolite levels in jejunum and plasma was observed for citrulline, serotonin, acylcarnitine and multiple species of phosphatidylcholines. Citrulline levels also correlated with injury and regeneration of crypts in the small intestine. These results expand the characterization of the natural history of gastrointestinal acute radiation syndrome in non-human primates exposed to partial body irradiation with minimal bone marrow sparing and also provide additional data toward the correlation of citrulline with histological endpoints.

[*]**Correspondence:** Maureen A. Kane, University of Maryland, School of Pharmacy, Department of Pharmaceutical Sciences, 20 N. Pine Street, Room N731, Baltimore, MD 21201, Phone: (410) 706-5097, Fax: (410) 706-0886, mkane@rx.umaryland.edu.
[+]contributed equally to this work

Conflicts of Interest:
Authors have no conflicts of interest to declare

INTRODUCTION

Exposure to high dose irradiation following a nuclear or radiological incident will result in the acute radiation syndromes (ARS) of the gastrointestinal (GI-ARS) and hematopoietic (H-ARS) systems in a dose-and time-dependent manner. Delayed effects of acute radiation exposure (DEARE) that includes multiorgan injury follow the ARS. Each resulting sequelae may be associated with high morbidity and mortality (MacVittie et al. 2012, MacVittie et al. 2012). Due to its rapidly proliferating cell populations, the GI is particularly susceptible to ARS (Potten 1990). Characteristics of the injury include damage to the mucosal layer of the small intestine, loss of clonogenic crypt cells, villus blunting, and barrier disruption accompanied by weight loss, diarrhea, dehydration, reduced nutrient absorption and intestinal infection (Booth and Potten 2002). Identification of circulating plasma biomarkers indicative of GI-ARS can be useful for early triage and injury assessment, and in the development of novel therapies (medical countermeasures). Currently, there is no drug approved for the GI-ARS by the Food and Drug Administration (FDA) (Rios et al. 2014). There also are no FDA qualified metabolite biomarkers available for any radiation injury.

Development of medical countermeasures to mitigate radiation-induced injury requires well developed animal models and occurs according to the FDA's animal rule. The FDA animal rule allows approval of medical countermeasures based on well controlled animal studies, when human clinical studies are not ethical or feasible (FDA 2015, FDA 2020). An analysis of biomarkers is an expectation of natural history studies as defined under the FDA animal rule. Evaluation of potential treatment triggers and/or definition of critical determinants of the natural history include biomarkers; biomarkers are also indicated to be relevant to human dose selection based upon biomarker levels established in well-defined animal models (FDA 2015). A key aspect of biomarkers is the biomarker-clinical endpoint relationship which is part of defining a biomarker's specific use and interpretable meaning during drug development (Califf 2018). Clinical endpoints can include, but are not limited to, histological analyses, functional assays, imaging analyses, and survival.

Biomarkers in an accessible biofluid are most desirable and practical. A variety of approaches have been applied to the identification and quantification of radiation biomarkers (Jones JW 2014). Studying the alterations in the metabolome at the target tissue site allows for the study of mechanism and extent of injury as metabolites are downstream products of cellular function and the injury to the tissues can alter metabolite levels multiple fold. Complementary interrogation of target tissue and plasma allows for the evaluation of tissue-plasma correlations (Jones et al. 2019). Assessment of metabolite changes at the target tissue site in a NHP model for GI injury is limited (Cheema et al. 2019). Citrulline is the metabolite that has been characterized most thoroughly for the GI-ARS (Jones et al. 2015, Jones et al. 2015, Bujold et al. 2016, Jones et al. 2019).

The partial body irradiation (PBI) with minimal, 2.5% or 5%, bone marrow (BM) sparing NHP model was developed to mimic intentional or accidental radiation exposures in humans. Such exposures are likely to include bone marrow sparing and to permit the concurrent analysis of coincident short- and long-term damage to organ systems in a time

and dose dependent manner (MacVittie et al. 2012). Previous publications by our team have described this PBI model, the analysis of resulting tissue injury, as well as its use for medical countermeasure development (MacVittie et al. 2012, Jones et al. 2015, MacVittie et al. 2015, Shea-Donohue et al. 2016, Cohen et al. 2017, Prado et al. 2017, Carter et al. 2019, Cohen et al. 2019, Farese et al. 2019, MacVittie et al. 2019, MacVittie et al. 2019, Parker et al. 2019, Parker et al. 2019, Parker et al. 2019).

Here, we sought to further characterize the natural history of the GI-ARS in NHP via determination of changes in the metabolite levels in jejunum and plasma. A more in-depth characterization of the natural history of radiation-induced damage in NHPs exposed to PBI with minimal BM sparing, including the establishment of tissue-plasma correlations of potential biomarkers as well as correlations with histological endpoints, increases the usefulness of the model for medical countermeasure development as understanding of the natural history of an injury is a general expectation of drug development under the FDA Animal Rule (FDA 2015).

MATERIALS AND METHODS

Radiation animal model.

All animal procedures were conducted in accordance with the NIH guidelines for the care and use of laboratory animals and experiments were performed with prior approval from the University of Maryland Institutional Animal Care and Use Committee (IACUC). Plasma was obtained from EDTA- anticoagulated peripheral blood of male rhesus macaques (*Macaca mulatta*); tissue was collected from a similar region of the jejunum and tissues were snap frozen in liquid nitrogen. Plasma and tissues were stored at −80 °C until assay. Samples were provided by the laboratory of Thomas J. MacVittie, University of Maryland School of Medicine, Department of Radiation Oncology (Baltimore, MD). Description of the animal models, including radiation exposure and dosimetry, medical management (supportive care and health monitoring), as well as collection of tissue have been previously described (MacVittie et al. 2012). Briefly, NHP [5.5 – 11.3 kg body weight] were exposed to either 12 Gy partial body irradiation with 2.5% bone marrow sparing (PBI/BM 2.5) (natural history study) or 10 Gy PBI/BM 2.5 (longitudinal study) with 6 MV LINAC-derived photons at 0.80 Gy min^{-1}. Bone marrow sparing was accomplished with tibiae outside the beam field. Plasma and jejunum were obtained from a natural history study (12 Gy PBI/BM 2.5) where timed euthanasia was planned at day 4 (n=4), 8 (n=7),11 (n=3), 15(n=5), and 21(n=3) after radiation. Additional plasma samples were obtained from animals that were euthanized according to criteria specified in the IACUC protocol. Plasma and tissue from non-irradiated animals (n=3) were used as baseline controls. Plasma from a longitudinal study (10 Gy PBI/BM 2.5) drawn post radiation at day 1(n=10), day 3 (n=10), day 7 (n=9), day 15 (n=9), day 21 (n=8), day 77 (n=5) and on day of morbidity (10) was also analyzed. Plasma from non-irradiated animals (n=10) were used as baseline controls

High Throughput, Targeted Metabolomics

Targeted, quantitative metabolomics was performed using Biocrates AbsoluteIDQ p180 kit (Biocrates, Life Science AG,Innsbruck,Austria). The AbsoluteIDQp180kit was prepared as

described by the manufacturer. The kit is a combined flow injection analysis (FIA) and liquid chromatography (LC) tandem mass spectrometry (MS) assay. The assay quantifies up to 188 metabolites from five metabolite classes: acylcarnitines, amino acids, biogenic amines, glycerophospholipids, sphingolipids, and hexose. Internal standards, analyte derivatization and metabolite extraction are integrated into a 96well plate kit. Metabolite detection is done via pre-selected multiple reaction monitoring (MRM) transitions. Briefly, jejunum tissue was snap frozen at the time of collection and stored at 80°C until analysis. Tissue was homogenized in 85:15 (methanol:ethanol, v/v) with 5 mM PBS at a ratio of 5 mg mL^{-1}. After centrifugation, 20 μL was loaded onto the 96 well kit plate and dried under a stream of nitrogen. A 5% solution of phenylisothiocyanate in ethanol:water:pyridine (1:1:1, v/v/v) was added for derivatization of biogenic amines and amino acids. Metabolite extraction was then achieved with 5 mM ammonium acetate in methanol. The FIA and LC tandem mass spectrometry platform consisted of a Waters I-Class UPLC coupled to a Waters TQ-S tandem quadrupole mass spectrometer. The MetIQ software (Biocrates) controlled the assay workflow including sample registration, calculation of metabolite concentrations, and assay validation. In the case of plasma samples 10 μL was used. Mobile phases used were of LC MS grade and all other reagents were of analytical grade.

Lipid annotation

PCs are phosphotidylcholines where “aa” indicates that fatty acids are bound to glycerol backbone via ester bonds at sn-1 position and bound to glycerol backbone via ester bonds at “sn-2” position, whereas “ae” indicates that fatty acids at sn-1 position are bound by ether bonds and are bound to glycerol backbone via ester bonds at “sn-2” position. The total number of carbon atoms and double bonds present in fatty acid chains are denoted as “C x:y”, where x is the number of carbons and y is the number of double bonds.

Data analysis

Data were exported to MetaboAnalyst (v4.0) (Chong et al. 2019), autoscaled and analyzed using statistical analysis and pathway enrichment analysis module. Box plots represent concentrations of selected metabolites and the black dots represent concentration of each sample. Mean concentration of each group is indicated by diamond shape and the notch indicate median of each group. Upper and lower extremes indicate 95% confidence interval around median of each group. Correlation analysis was performed against corrected crypt number time-series pattern. A distance measure of Spearman rank correlation was used. Quantitative pathway enrichment and pathway topology analysis was performed using metabolites concentration levels. Globaltest enrichment analysis was chosen to identify most relevant pathways in human KEGG library. Human library was chosen under the assumption that human pathway library are similar to rhesus macaques. P value is calculated from enrichment analysis. Lipid pathway enrichment analysis (Acevedo et al. 2018) was performed with most altered lipids to find relevant pathways applying Fisher’s exact test. Rhesus monkey pathway library was chosen. Enriched pathways with p – value was obtained as results.

Histological analyses.

Corrected crypt number as an index of crypt survival was measured as described previously (MacVittie et al. 2012). Briefly, samples of small intestine were collected at necropsy and fixed in formalin, embedded in paraffin, cut and mounted, and stained with hematoxylin and eosin (H&E). The number of surviving and regenerating crypts per length of intestine was scored and the average per group is calculated. The size of surviving crypts varied which influenced the likelihood of surviving crypt in cross section, so a size correction factor was applied to reduce this error based on widths of crypts in nonirradiated control NHPs and surviving crypts in irradiated NHPs. The corrected number of crypts was calculated according to the following equation: Corrected number of crypts = (mean width in control mice / mean width in irradiated mouse) x mean number of surviving crypts in the irradiated mouse.

RESULTS

Study design.

Non-human primates exposed to either 12 Gy PBI/BM 2.5 (natural history study) or 10 Gy PBI/BM 2.5 (longitudinal study) were assessed to identify potential biomarkers that have jejunum – plasma correlations and that also correlated with histological endpoints for GI-ARS. In the natural history study, plasma and jejunum samples were collected from various time points between day 0 to day 21 encompassing a time period containing the GI – ARS. In the longitudinal study, plasma samples were collected at various timepoints between day 0 and day until death, as long as 183 days. This duration included the GI-ARS and the time period of prolonged GI injury (GI – DEARE). Previous publications have described this PBI model and the analysis of resulting tissue injury (MacVittie et al. 2012, Jones et al. 2015, Shea-Donohue et al. 2016, Cohen et al. 2017, Prado et al. 2017, Carter et al. 2019, Cohen et al. 2019, MacVittie et al. 2019, MacVittie et al. 2019, Parker et al. 2019, Parker et al. 2019, Parker et al. 2019). Here we sought to further characterize the natural history of the GI-ARS in NHP via determination of differential metabolite and lipid abundance in plasma and jejunum. Additionally, we considered the metabolites and lipids yielded by our data towards supporting efforts to identify biomarkers that could have utility toward identification of exposed populations, and may be useful during drug development under the FDA Animal Rule, or inform on medical management of radiation-induced injuries post-exposure. Histological analysis of the jejunum to assess the extent of GI damage was performed as part of the natural history of 12 Gy PBI/BM 2.5. Corrected crypt number declined after radiation indicating a loss of crypt cells that was maintained to three weeks (Fig. 1). Regeneration of crypts at later time points (day 11, 15, 21) shows hyperplastic crypts that are larger than day 0. This same histological index that was used to evaluate the potential for metabolite biomarker candidates to inform on the GI-ARS was also used to evaluate the potential for protein biomarker candidates to inform on the GI-ARS in another manuscript in this issue (Huang et al. 2020)(Huang, et al.).

Plasma-tissue correlations across the natural history of the GI-ARS

Over 180 metabolite levels and relevant biological ratios were quantified in plasma and jejunum as part of the natural history study after 12 Gy PBI/BM 2.5 (Supplemental Table

S1, Supplemental Table S2). Metabolites were filtered for those that had correlation with the temporal patterns of corrected crypt number (Fig. 1a) as well as a correlation between jejunum and plasma levels (Fig. 2–4). As expected according to our previous work, citrulline was decreased after radiation and had a similar temporal response in both jejunum and plasma (Fig. 2). Jejunum citrulline increased in levels after day 8 and had levels higher than baseline on day 21. Plasma citrulline also began to increase after day 8, but did not return to baseline by day 21. Two other metabolites, serotonin, acylcarnitine C18, were also decreased after radiation and had a similar temporal response in both jejunum and plasma (Fig. 3). Multiple phosphotidylcholine species had similar jejunum and plasma temporal profiles that were similar to the temporal profile of corrected crypt number. These lipids decreased after radiation and included (PC ae C34:2, PC ae C34:3, PC ae C36:2, PC ae C36:3, PC ae C38:1, and PC ae C38:2 (Fig. 4).

Correlation with histological endpoints

Jejunum and plasma metabolite levels were correlated with corrected crypt number, a well-characterized histological endpoint for the GI-ARS, after 12 Gy PBI/BM 2.5. Radiation induces loss of crypts and after four days post-irradiation, a drastic reduction in number of crypts was observed with a nadir at day 8 (Fig. 1a). On days 11, 15, and 21 there is an increase in corrected crypt number marking a degree of recovery of intestinal lining, albeit corrected crypt number remains still markedly reduced from baseline (Fig. 1a). Whereas, the corrected crypt number has been shown to be a highly effective way to assess the GI-ARS (Booth et al. 2012, MacVittie et al. 2012), there is still a need for less invasive parameters that have the ability to assess GI injury with similar effectiveness to corrected crypt number. The correlation between jejunum metabolite levels and corrected crypt number is shown in Table 1. The correlations ranged from 0.30 (acylcarnitine C18) to 0.76 (PC ae 36:3). Citrulline, serotonin, PC ae 34:2, PC ae 34:3, PS ae 36:2, PC ae 36:3, PC ae 38:1, and PC ae 38:2 had statistically significant jejunum-corrected crypt number correlations (Table 1). The correlation between plasma metabolite levels and corrected crypt number is shown in Table 2. Many of the plasma metabolite levels had weaker correlations with corrected crypt number with only citrulline having a statistically significant correlation with corrected crypt number (0.67) (Table 2).

Longitudinal plasma characterization including the GI-ARS and the prolonged GI injury

To test the repeatability of response during the GI-ARS for the metabolites identified in Fig. 2–4 as well as to determine their response during prolonged GI injury, plasma from a longitudinal study of 10 Gy PBI/BM 2.5 was assayed (Supplemental Table S3). Plasma metabolite levels were assayed at timepoints up until day 183 (Fig. 5). The day of death in the longitudinal study ranged between day 14 to day 183 (mean survival was 84 days for the samples assayed in the longitudinal study) (Supplemental Table S4). The metabolites and lipids from the longitudinal study of plasma samples after 10Gy PBI/BM 2.5 were selected for a temporal pattern that matches with the response in plasma after 12 Gy PBI/BM 2.5. In the longitudinal study, levels of citrulline and phosphotidylcholines (PC ae C38:2, PC ae C36:2, PC ae C34:3) decreased post-irradiation similar to that observed in the 12 Gy PBI/BM 2.5 natural history study (Fig. 5). Citrulline increased at later timepoints after

radiation, whereas all of the lipid species (PC ae 34:3, PC ae 36:2, PC ae 36:3, and PC ae 38:2) remained depressed throughout the study (Fig. 5).

Pathway analysis to inform on the GI-ARS mechanisms of injury

In order to understand the mechanism of injury and its influence on metabolism, we performed pathway analysis of metabolites (Fig. 6) and lipids (Table 3) by comparing day 0 and day 4 metabolite levels from the natural history study. Quantitative pathway enrichment and topology analysis of jejunum and plasma indicates dysregulation of amino acid metabolism and regulation consistent with dysfunction of GI homeostasis (Fig. 6). A number of phosphotidylcholine lipids consistently and robustly changed after radiation. As such, we performed lipid pathway enrichment analysis to gain insight into the associated pathways that are dysregulated by altered phosphotidylcholine species after 12 Gy PBI/BM 2.5 (Table 3). These pathways included those related to choline, endocannabinoid, linolenic acid, linoleic acid, arachidonic acid, and glycerophospholipid metabolism (Table 3).

DISCUSSION

In this study, we used liquid chromatography-tandem mass spectrometry to identify radiation-responsive metabolites and lipids in plasma and jejunum that correlated with an established histological endpoint for the GI-ARS. Histological analyses, including corrected crypt number, have been rigorously developed to assess and characterize the natural history of the GI-ARS in both mouse and NHP (Booth et al. 2012, Booth et al. 2012, MacVittie et al. 2012, MacVittie et al. 2012, MacVittie et al. 2019). Corrected crypt number is a histological index of GI injury that has been used to evaluate biomarkers and their ability to corelate with well-characterized endpoints of GI injury (Jones et al. 2015, Jones et al. 2015). We observed a decrease in corrected crypt number after radiation consistent with previous assessments of radiation-induced GI damage in NHP after PBI (MacVittie et al. 2012). The tissue-plasma correlations reported here in primate share similarities to the tissue-plasma correlations that we observed in a mouse model of the GI-ARS previously which included citrulline, PC ae 36:2, and PC ae 38:2 (Jones et al. 2019).

Citrulline, a non-essential amino acid, is an end product of glutamine metabolism by small intestinal enterocytes. Multiple enzymes – Ornithine aminotransferase (OAT), Ornithine Carbamoyltransferase (OCT), Carbomyl phosphate synthetase I (CPSI), Proline oxidase (PROox) and Pyrroline-5-carboxylante synthase (P5cs) that are exclusively present in small intestinal enterocytes synthesize citrulline from glutamine and/or proline. In a parallel proteomic study after 12 Gy PBI/BM 2.5, also published in this issue, we observed significant decrease in OAT after radiation which may contribute to the observed citrulline deficiency (Huang et al. 2020)(Huang, et al.). Under steady state conditions, rate of citrulline released into portal and subsequently the systemic circulation correlates with the actual number of cell mass that is present in small bowel epithelium. Therefore, circulating plasma citrulline can be a marker for functional epithelial mass (Lutgens and Lambin 2007). In human, 20 μM of plasma citrulline is considered as a best threshold for permanent intestinal failure with a sensitivity, specificity, positive predictive value (PPV) and negative predictive value (NPV) of 92%, 90%, 95% and 85% respectively. Fig. 2 shows plasma citrulline levels

are below this threshold in NHP after 12 Gy PBI/BM 2.5. Citrulline also serves as a marker for intestinal absorption and function. Lower level may indicate damage to small intestinal epithelium, small intestinal absorption and function (Fragkos and Forbes 2018). About 80% of citrulline is transported to be metabolized by the kidney for arginine synthesis, nitric oxide (NO) production in vascular epithelium and as well metabolized by the urea cycle (Barzał et al. 2014). Previously, we reported the ability of citrulline as plasma biomarker in NHP model after TBI at 13.0 Gy, 10.5 Gy, and 7.5 Gy and PBI at 11.0 Gy with 5% bone marrow sparing (Jones et al. 2015) and correlation of tissue and plasma levels in murine models post TBI exposure of 6 – 15 Gy (Jones et al. 2015), and developed a quantitation method for measuring citrulline (Jones et al. 2014). In mice, after a single TBI of 1 – 12Gy dosage, citrulline levels were most reduced at 3.5 to 4 days post radiation (Lutgens et al. 2003). Another study evaluating species differences and experimental conditions like feeding and anesthesia on citrulline as biomarker, exposed mice and minipigs to PBI with doses from 13–17 Gy and 8–16 Gy, respectively and NHP to TBI with doses from 6.72–13 Gy. It was reported that in NHP, plasma citrulline levels reached nadir values between days 3.5 and 7 days(Bujold et al. 2016). Here, we report tissue-plasma correlation of citrulline in NHP model after PBI, further validating the utility and reliability of citrulline as a biomarker for small intestinal epithelial damage. Both, plasma and jejunum citrulline levels reach nadir levels on day 8 post radiation. Alterations in citrulline levels impact arginine biosynthesis which is consistent with the pathway analysis (Fig. 6b).

Serotonin, a neurotransmitter and signaling molecule is synthesized from tryptophan by tryptophan hydroxylase, which is an enzyme present in Enterochromaffin (EC) cells. About 90% of body serotonin is found in EC cells (Sikander et al. 2009). EC cells reside alongside epithelial lining located in crypts between intestinal villi of GI tract lumen and play a crucial role in intestinal motility and secretion. EC cells are discriminated from other cell epithelial crypts by the presence of basally located granulations having serotonin and other peptides (Wade and Westfall 1985). Alterations in serotonin impacts tryptophan metabolism which is shown in the pathway analysis of jejunum (Fig. 6a) and plasma (Fig. 6b). Previously, we reported a study in mouse total body irradiation model, where after exposure to radiation above 8Gy, serotonin levels decreased in jejunum(Jones et al. 2019).

Intestinal epithelium is protected by a mucus layer that is hydrophobic. Its hydrophobicity is largely due to phospholipids (Lugea et al. 2000). About 90% of phospholipids in mucus layer are phosphatidylcholines (Stremmel et al. 2016). It has been noted that phospholipids can protect against apoptosis in epithelial cells (Leucht et al. 2014). Membrane phospholipids, especially those with a more oxidatively labile ether linkage, are targets of reactive oxygen species (ROS) formed due to ionizing radiation which may have led to alterations in our observed ether-linked phosphatidylcholine levels (Jones et al. 2017). PC ae 36:3 and PC ae 38:2 were also reduced in the jejunum in a study of NHP exposed to gamma-radiation (Cheema et al. 2019). The highlighted lipid species remain depressed throughout the longitudinal study which may indicate persistent dysfunction in NHP GI at longer time post-radiation consistent with previous reports (MacVittie et al. 2012). The impact of the lipid depletion observed here warrants further study as the metabolic pathways that are affected by altered phosphatidylcholine levels are important to GI homeostasis (Table 3). In another study, mice were exposed to a dose of 8Gy and multiple ether phosphatidylcholine

species were found to be upregulated in serum of radiated animals, on contrary to the observation in NHP plasma and tissues in this study(Laiakis et al. 2014).

CONCLUSION

Plasma and jejunum metabolites were quantified via liquid chromatography - tandem mass spectrometry and histological analysis consisted of corrected crypt number, an established metric to assess radiation-induced gastrointestinal damage. A positive correlation of metabolite levels in jejunum and plasma was observed for citrulline, serotonin, acylcarnitine and multiple species of phosphatidylcholines. Citrulline levels also correlated with injury and regeneration of crypts in the small intestine. Alteration in serotonin levels indicate dysfunction of EC cells and alteration in PC levels is consistent with mucosal damage in the jejunum. These results expand the characterization of the natural history of the GI-ARS in NHP exposed to PBI with minimal bone marrow sparing and also provide additional data toward the correlation of citrulline with histological endpoints.

Supplementary Material

Refer to Web version on PubMed Central for supplementary material.

ACKNOWLEDGEMENTS

This project has been funded in whole or in part with Federal funds from the National Institute of Allergy and Infectious Diseases, National Institutes of Health, Department of Health and Human Services, under Contract No. HHSN272201000046C and HHSN272201500013I. Additional support was provided by the University of Maryland School of Pharmacy Mass Spectrometry Center (SOP1841-IQB2014).

REFERENCES

Acevedo A, Duran C, Ciucci S, Gerl M, Cannistraci CV. Lipea: Lipid pathway enrichment analysis. bioRxiv: 274969; 2018.

Barzał JA, Szczylik C, Rzepecki P, Jaworska M, Anuszewska E. Plasma citrulline level as a biomarker for cancer therapy-induced small bowel mucosal damage. Acta Biochimica Polonica 61; 2014.

Booth C, Potten CS. The intestine as a model for studying stem-cell behavior In: Teichers BA ed. Tumor models in cancer research. Totowa, NJ: Humana Press; 2002; 337–357.

Booth C, Tudor G, Tonge N, Shea-Donohue T, MacVittie TJ. Evidence of delayed gastrointestinal syndrome in high-dose irradiated mice. Health Phys 103: 400–10; 2012. [PubMed: 23091877]

Booth C, Tudor G, Tudor J, Katz BP, MacVittie TJ. Acute gastrointestinal syndrome in high-dose irradiated mice. Health Phys 103: 383–99; 2012. [PubMed: 23091876]

Bujold K, Hauer-Jensen M, Donini O, Rumage A, Hartman D, Hendrickson HP, Stamatopoulos J, Naraghi H, Pouliot M, Ascah A, Sebastian M, Pugsley MK, Wong K, Authier S. Citrulline as a biomarker for gastrointestinal-acute radiation syndrome: Species differences and experimental condition effects. Radiat Res 186: 71–8; 2016. [PubMed: 27351760]

Califf RM. Biomarker definitions and their applications. Exp Biol Med (Maywood) 243: 213–221; 2018. [PubMed: 29405771]

Carter CL, Hankey KG, Booth C, Tudor GL, Parker GA, Jones JW, Farese AM, MacVittie TJ, Kane MA. Characterizing the natural history of acute radiation syndrome of the gastrointestinal tract: Combining high mass and spatial resolution using maldi-fticr-msi. Health Phys; 2019.

Cheema AK, Mehta KY, Rajagopal MU, Wise SY, Fatanmi OO, Singh VK. Metabolomic studies of tissue injury in nonhuman primates exposed to gamma-radiation. Int J Mol Sci 20; 2019.

Chong J, Wishart DS, Xia J. Using metaboanalyst 4.0 for comprehensive and integrative metabolomics data analysis. Current protocols in bioinformatics 68: e86; 2019. [PubMed: 31756036]

Cohen EP, Hankey KG, Bennett AW, Farese AM, Parker GA, MacVittie TJ. Acute and chronic kidney injury in a non-human primate model of partial-body irradiation with bone marrow sparing. Radiat Res 188: 661–671; 2017. [PubMed: 29035153]

Cohen EP, Hankey KG, Farese AM, Parker GA, Jones JW, Kane MA, Bennett A, MacVittie TJ. Radiation nephropathy in a nonhuman primate model of partial-body irradiation with minimal bone marrow sparing-part 1: Acute and chronic kidney injury and the influence of neupogen. Health Phys 116: 401–408; 2019. [PubMed: 30608245]

Farese AM, Bennett AW, Gibbs AM, Hankey KG, Prado K, Jackson W 3rd, MacVittie TJ. Efficacy of neulasta or neupogen on h-ars and gi-ars mortality and hematopoietic recovery in nonhuman primates after 10-gy irradiation with 2.5% bone marrow sparing. Health Phys 116: 339–353; 2019. [PubMed: 30281533]

FDA. Product development under the animal rule: Guidance for industry. 2015.

FDA. Product development under the animal rule: Guidance for industry. [online]. Available at: https://www.fda.gov/downloads/drugs/guidances/ucm399217.pdf.

FDA. Animal rule information [online]. Available at: https://www.fda.gov/emergency-preparedness-and-response/mcm-regulatory-science/animal-rule-information. Accessed 04/29.

Fragkos KC, Forbes A. Citrulline as a marker of intestinal function and absorption in clinical settings: A systematic review and meta-analysis. United European gastroenterology journal 6: 181–191; 2018. [PubMed: 29511548]

Huang W, Yu J, Liu T, Tudor G, Defnet AE, Zalesak S, Kumar P, Booth C, Farese AM, MacVittie TJ, Kane MA. Proteomic evaluation of the acute radiation syndrome of the gastrointestinal tract in anonhuman primate model of partial-body irradiation with minimal bone marrow sparing. Health Phys; 2020.

Jones JW, Bennett A, Carter CL, Tudor G, Hankey KG, Farese AM, Booth C, MacVittie TJ, Kane MA. Citrulline as a biomarker in the non-human primate total- and partial-body irradiation models: Correlation of circulating citrulline to acute and prolonged gastrointestinal injury. Health Phys 109: 440–51; 2015. [PubMed: 26425904]

Jones JW, Bennett A, Carter CL, Tudor G, Hankey KG, Farese AM, Booth C, MacVittie TJ, Kane MA. Citrulline as a biomarker in the non-human primate total-and partial-body irradiation models: Correlation of circulating citrulline to acute and prolonged gastrointestinal injury. Health Phys 109: 440; 2015. [PubMed: 26425904]

Jones JW, Clifford Z, Li F, Tudor GL, Farese AM, Booth C, MacVittie TJ, Kane MA. Targeted metabolomics reveals metabolomic signatures correlating gastrointestinal tissue to plasma in a mouse total-body irradiation model. Health Phys 116: 473–483; 2019. [PubMed: 30624349]

Jones JW, Clifford Z, Li F, Tudor GL, Farese AM, Booth C, MacVittie TJ, Kane MA. Targeted metabolomics reveals metabolomic signatures correlating gastrointestinal tissue to plasma in a mouse total-body irradiation model. Health Phys; 2019.

Jones JW, Jackson IL, Vujaskovic Z, Kaytor MD, Kane MA. Targeted metabolomics identifies pharmacodynamic biomarkers for bio 300 mitigation of radiation-induced lung injury. Pharmaceutical research 34: 2698–2709; 2017. [PubMed: 28971289]

Jones JW SA, Tudor G, Xu PT, Jackson IL, Vujaskovic Z, Booth C, MacVittie TJ, Ernst RK, Kane MA. Identification and quantitation of biomarkers for radiation-induced injury via mass spectrometry. Health Phys 106: 106–19; 2014. [PubMed: 24276554]

Jones JW, Tudor G, Bennett A, Farese AM, Moroni M, Booth C, MacVittie TJ, Kane MA. Development and validation of a lc-ms/ms assay for quantitation of plasma citrulline for application to animal models of the acute radiation syndrome across multiple species. Analytical and bioanalytical chemistry 406: 4663–75; 2014. [PubMed: 24842404]

Jones JW, Tudor G, Li F, Tong Y, Katz B, Farese AM, MacVittie TJ, Booth C, Kane MA. Citrulline as a biomarker in the murine total-body irradiation model: Correlation of circulating and tissue citrulline to small intestine epithelial histopathology. Health Phys 109: 452; 2015. [PubMed: 26425905]

Jones JW, Tudor G, Li F, Tong Y, Katz B, Farese AM, MacVittie TJ, Booth C, Kane MA. Citrulline as a biomarker in the murine total-body irradiation model: Correlation of circulating and tissue citrulline to small intestine epithelial histopathology. Health Phys 109: 452–65; 2015. [PubMed: 26425905]

Laiakis EC, Strassburg K, Bogumil R, Lai S, Vreeken RJ, Hankemeier T, Langridge J, Plumb RS, Fornace AJ, Astarita G. Metabolic phenotyping reveals a lipid mediator response to ionizing radiation. Journal of Proteome Research 13: 4143–4154; 2014. [PubMed: 25126707]

Leucht K, Fischbeck A, Caj M, Liebisch G, Hartlieb E, Benes P, Fried M, Humpf HU, Rogler G, Hausmann M. Sphingomyelin and phosphatidylcholine contrarily affect the induction of apoptosis in intestinal epithelial cells. Molecular nutrition & food research 58: 782–798; 2014. [PubMed: 24142587]

Lugea A, Salas A, Casalot J, Guarner F, Malagelada JR. Surface hydrophobicity of the rat colonic mucosa is a defensive barrier against macromolecules and toxins. Gut 46: 515–521; 2000. [PubMed: 10716681]

Lutgens L, Lambin P. Biomarkers for radiation-induced small bowel epithelial damage: An emerging role for plasma citrulline. World J Gastroenterol 13: 3033–3042; 2007. [PubMed: 17589917]

Lutgens LC, Deutz NE, Gueulette J, Cleutjens JP, Berger MP, Wouters BG, von Meyenfeldt MF, Lambin P. Citrulline: A physiologic marker enabling quantitation and monitoring of epithelial radiation-induced small bowel damage. Int J Radiat Oncol Biol Phys 57: 1067–74; 2003. [PubMed: 14575838]

MacVittie TJ, Bennett A, Booth C, Garofalo M, Tudor G, Ward A, Shea-Donohue T, Gelfond D, McFarland E, Jackson W 3rd, Lu W, Farese AM. The prolonged gastrointestinal syndrome in rhesus macaques: The relationship between gastrointestinal, hematopoietic, and delayed multi-organ sequelae following acute, potentially lethal, partial-body irradiation. Health Phys 103: 427–53; 2012. [PubMed: 22929471]

MacVittie TJ, Bennett AW, Farese AM, Taylor-Howell C, Smith CP, Gibbs AM, Prado K, Jackson W 3rd. The effect of radiation dose and variation in neupogen(r) initiation schedule on the mitigation of myelosuppression during the concomitant gi-ars and h-ars in a nonhuman primate model of high-dose exposure with marrow sparing. Health Phys 109: 427–39; 2015. [PubMed: 26425903]

MacVittie TJ, Farese AM, Bennett A, Gelfond D, Shea-Donohue T, Tudor G, Booth C, McFarland E, Jackson W. The acute gastrointestinal subsyndrome of the acute radiation syndrome: A rhesus macaque model. Health Phys 103: 411–426; 2012. [PubMed: 22929470]

MacVittie TJ, Farese AM, Bennett A, Gelfond D, Shea-Donohue T, Tudor G, Booth C, McFarland E, Jackson W 3rd. The acute gastrointestinal subsyndrome of the acute radiation syndrome: A rhesus macaque model. Health Phys 103: 411–26; 2012. [PubMed: 22929470]

MacVittie TJ, Farese AM, Parker GA, Jackson W 3rd. The time course of radiation-induced lung injury in a nonhuman primate model of partial-body irradiation with minimal bone marrow sparing: Clinical and radiographic evidence and the effect of neupogen administration. Health Phys 116: 366–382; 2019. [PubMed: 30624350]

MacVittie TJ, Farese AM, Parker GA, Jackson W 3rd, Booth C, Tudor GL, Hankey KG, Potten CS. The gastrointestinal subsyndrome of the acute radiation syndrome in rhesus macaques: A systematic review of the lethal dose-response relationship with and without medical management. Health Phys 116: 305–338; 2019. [PubMed: 30624353]

Parker GA, Cohen EP, Li N, Takayama K, Farese AM, MacVittie TJ. Radiation nephropathy in a nonhuman primate model of partial-body irradiation with minimal bone marrow sparing-part 2: Histopathology, mediators, and mechanisms. Health Phys 116: 409–425; 2019. [PubMed: 30624348]

Parker GA, Li N, Takayama K, Booth C, Tudor GL, Farese AM, MacVittie TJ. Histopathological features of the development of intestine and mesenteric lymph node injury in a nonhuman primate model of partial-body irradiation with minimal bone marrow sparing. Health Phys 116: 426–446; 2019. [PubMed: 30624355]

Parker GA, Li N, Takayama K, Farese AM, MacVittie TJ. Lung and heart injury in a nonhuman primate model of partial-body irradiation with minimal bone marrow sparing: Histopathological evidence of lung and heart injury. Health Phys 116: 383–400; 2019. [PubMed: 30688698]

Potten CS. A comprehensive study of the radiobiological response of the murine (bdf1) small intestine. International Journal of Radiation Biology 58: 925–973; 1990. [PubMed: 1978853]

Prado C, MacVittie TJ, Bennett AW, Kazi A, Farese AM, Prado K. Organ doses associated with partial-body irradiation with 2.5% bone marrow sparing of the non-human primate: A retrospective study. Radiat Res 188: 615–625; 2017. [PubMed: 28985133]

Rios CI, Cassatt DR, Dicarlo AL, Macchiarini F, Ramakrishnan N, Norman MK, Maidment BW. Building the strategic national stockpile through the niaid radiation nuclear countermeasures program. Drug Dev Res 75: 23–8; 2014. [PubMed: 24648046]

Shea-Donohue T, Fasano A, Zhao A, Notari L, Yan S, Sun R, Bohl JA, Desai N, Tudor G, Morimoto M, Booth C, Bennett A, Farese AM, MacVittie TJ. Mechanisms involved in the development of the chronic gastrointestinal syndrome in nonhuman primates after total-body irradiation with bone marrow shielding. Radiat Res 185: 591–603; 2016. [PubMed: 27223826]

Sikander A, Rana SV, Prasad KK. Role of serotonin in gastrointestinal motility and irritable bowel syndrome. Clinica Chimica Acta 403: 47–55; 2009.

Stremmel W, Staffer S, Gan-Schreier H, Wannhoff A, Bach M, Gauss A. Phosphatidylcholine passes through lateral tight junctions for paracellular transport to the apical side of the polarized intestinal tumor cell-line caco2. Biochimica et biophysica acta 1861: 1161–1169; 2016. [PubMed: 27365309]

Wade PR, Westfall JA. Ultrastructure of enterochromaffin cells and associated neural and vascular elements in the mouse duodenum. Cell and Tissue Research 241: 557–563; 1985. [PubMed: 4028141]

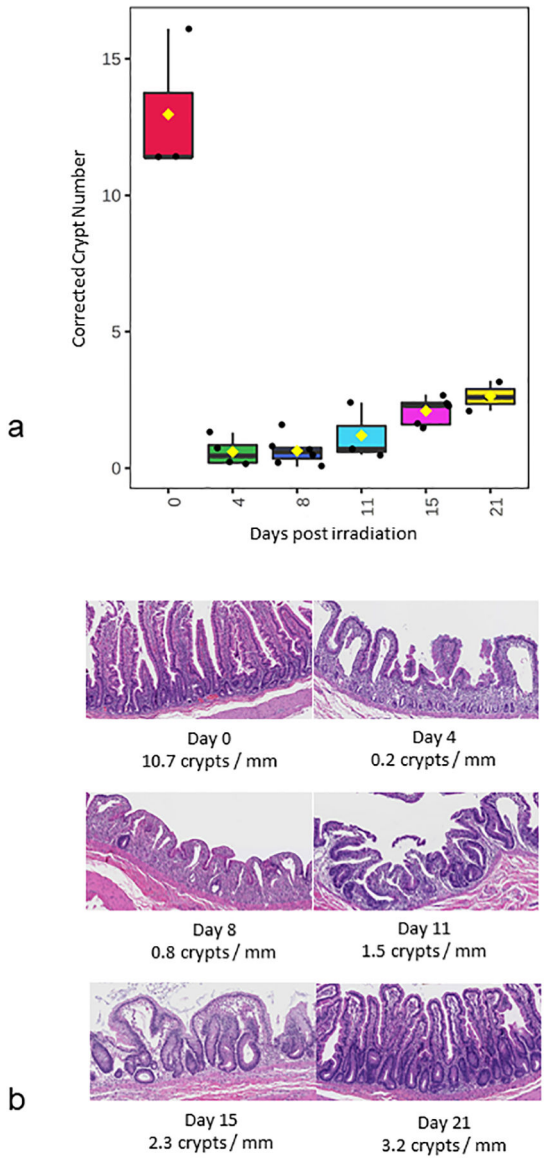

Figure 1. Histological analysis of NHP jejunum after 12 Gy PBI/BM 2.5 to assess GI damage.
(a) corrected crypt number, (b) representative H&E stained histology images.

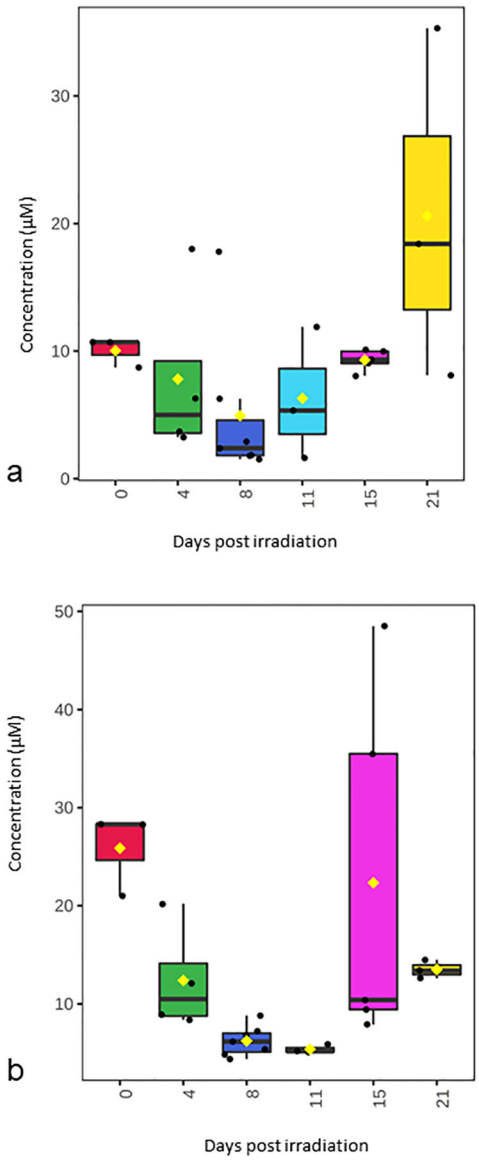

Figure 2. Temporal pattern of citrulline levels in jejunum and plasma after 12 Gy PBI/BM 2.5.
(a) jejunum citrulline, (b) plasma citrulline.

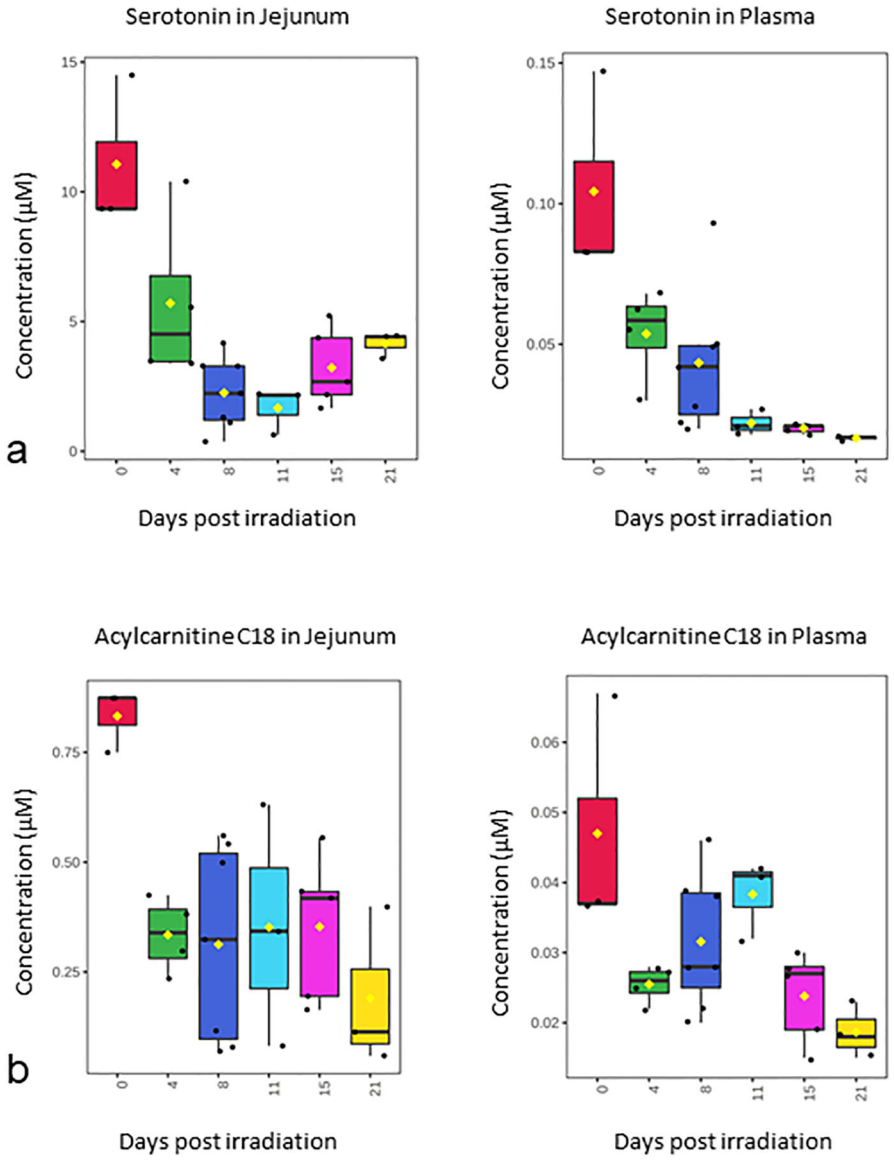

Figure 3. Temporal pattern of serotonin and acylcarnitine C18 in jejunum and plasma after 12 Gy PBI/BM 2.5.

(a) serotonin, (b) acylcarnitine C18.

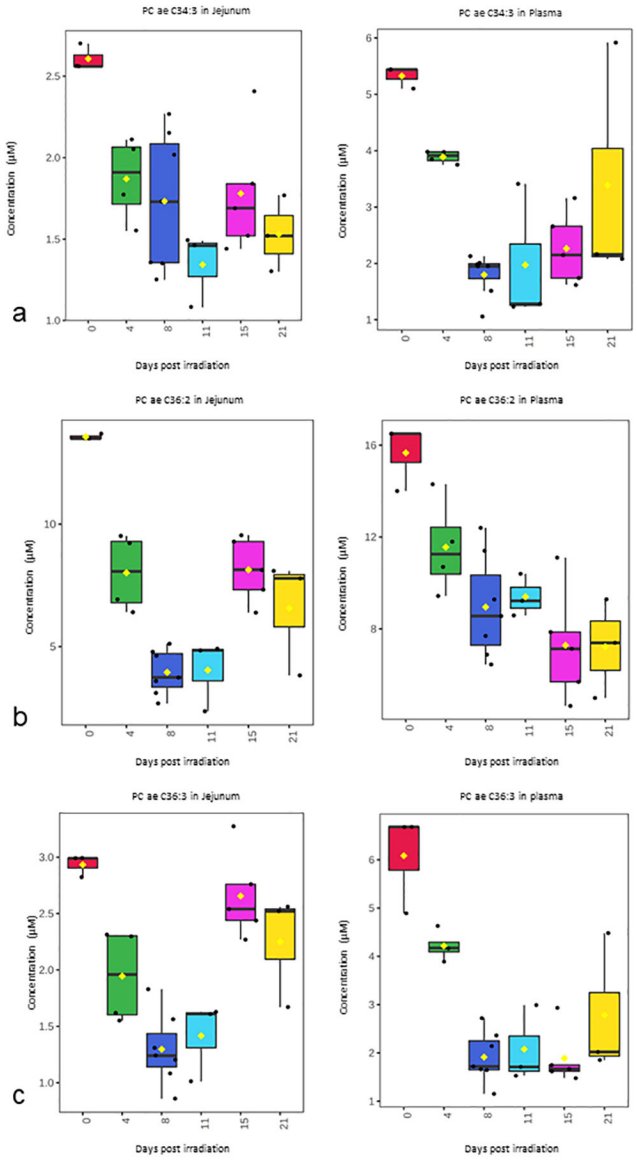

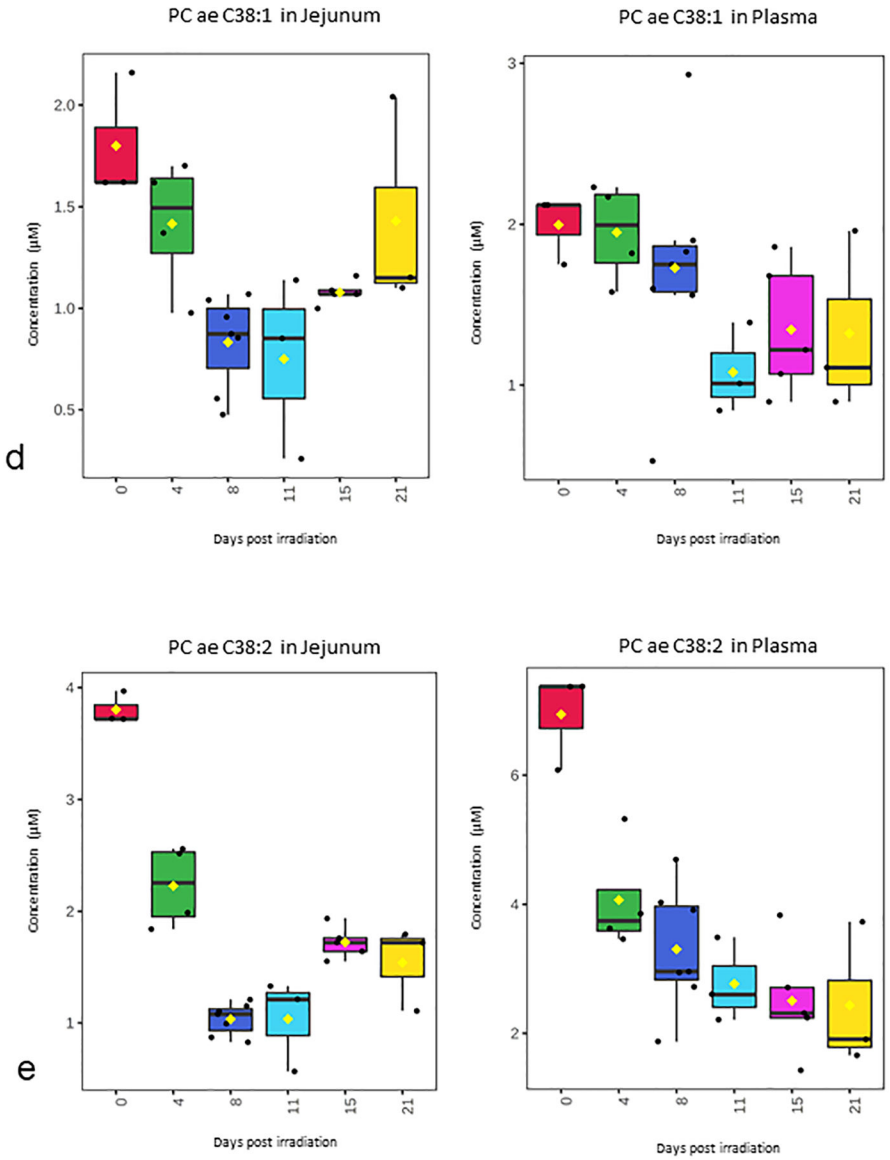

Figure 4. Temporal pattern of selected phosphotidylcholine species in jejunum and plasma after 12 Gy PBI/BM 2.5.

(a) PC ae C34:3, (b) PC ae C36:2, (c) PC ae C36:3, (d) PC ae C38:1, (e) PC ae C38:2

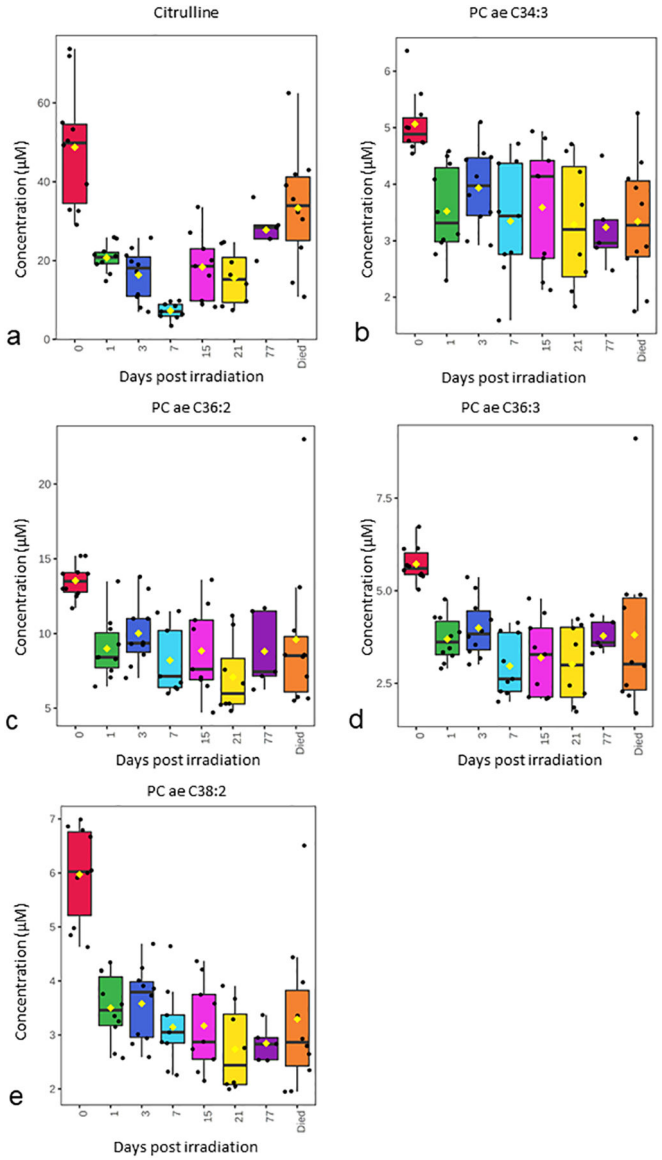

Figure 5. Selected temporal pattern of metabolites and lipids from longitudinal study of plasma samples after 10 Gy PBI/BM 2.5.

(a) Citrulline, (b) PC ae C34:3, (c) PC ae C36:2, (d) PC ae C36:3, (e) PC ae C38:2

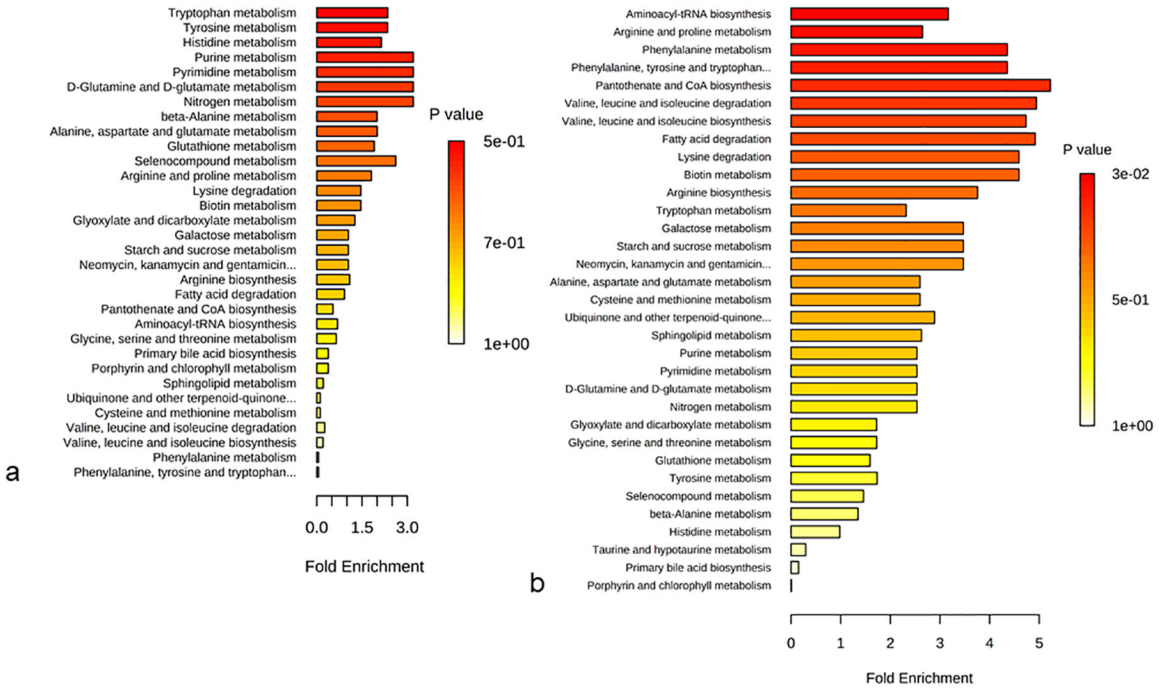

Figure 6. Quantitative pathway enrichment and topology analysis of metabolite alterations in jejunum and plasma after 12 Gy PBI/BM 2.5.

Analysis comparing day 0 and day 4 for (a) jejunum, (b) plasma.

Table 1.

Correlation of jejunum levels and corrected crypt number

Correlation with corrected crypt number		
Analyte	**R**	**p-value**
PC ae C36:2	0.62	0.0010
PC ae C38:1	0.60	0.0015
PC ae C38:2	0.52	0.0073
PC ae C34:3	0.35	0.0902
PC ae C34:2	0.66	0.0004
PC ae C36:3	0.76	<0.0001
Serotonin	0.42	0.0344
Acylcarnitine C18	0.30	0.1451
Citrulline	0.54	0.0051

Table 2.

Correlation of plasma levels and corrected crypt number

Correlation with corrected crypt number		
Analyte	**R**	**p-value**
PC ae C36:2	0.18	0.3850
PC ae C38:1	0.11	0.6119
PC ae C38:2	0.20	0.3481
PC ae C34:3	0.35	0.0839
PC ae C34:2	0.23	0.2783
PC ae C36:3	0.28	0.1747
Serotonin	−0.07	0.7532
Acylcarnitine C18	0.05	0.7965
Citrulline	0.67	0.0003

Table 3.

Pathways affected by altered phosphotidylcholine levels after 12 Gy PBI/BM 2.5.

Pathway name	p-value	Benjamini correction
Choline metabolism in cancer	0.009	0.045
Retrograde endocannabinoid signaling	0.015	0.045
alpha-Linolenic acid metabolism	0.043	0.058
Linoleic acid metabolism	0.047	0.058
Glycerophospholipid metabolism	0.049	0.058
Arachidonic acid metabolism	0.140	0.140